



AESTHETIC FACIAL ANALYSIS

|| Marc S. Zimbler
|| Jongwook Ham

INTRODUCTION

Throughout history mankind has tried to define beauty. Poets, philosophers, and artists have pondered its elusive quality while attempting to quantify that which is evident to all of us. As surgeons, however, we are required to have a more scientific approach to beauty to formulate operative plans with successful surgical outcomes. Common reference points are essential in communicating with colleagues and medical record keeping. Furthermore, we must be able to accurately define specific characteristics that deviate from the norm so that we may identify congenital anomalies and facial deformities.

As early as ancient Egypt, aesthetic facial proportions have been idealized in art. However, it was not until the Greek philosophers that the study of beauty became a formal discipline. To Plato and Aristotle beauty meant symmetry, harmony, and geometry. In the fifth century BC, the Greek sculptor Polyclitus defined perfect beauty as the mutual harmony of all parts, such that nothing could be added or subtracted. Such harmonic proportions were held to be beautiful in themselves, independent of any observer.

These ideas were later revisited by the Renaissance artists, who began to define ideal proportions for the human form. This example is nowhere more evident than in the drawings of Leonardo da Vinci and his Vitruvian man (Figure 21-1). It was da Vinci, who, through the study of anatomy, formulated ideal facial proportions and divided the profile into equal thirds (Figure 21-2). Leonardo's scientific accuracy rivaled that of Vesalius, whereas his artistic beauty remains unchallenged. Another Renaissance artist inspired by the Vitruvian notion of perfect proportions was the German printmaker Albrecht Durer. Durer used his own finger as a unit of measurement to construct a proportional system for the entire body, and in 1528 he published a four-book treatise on human proportions. Durer divided the facial profile into four equal parts and recognized that the length of the nose equals that of the ear.

The artistic cannons set forth in antiquity and during the Renaissance dominated Western art for centuries. In the twentieth century, anthropometrist Leslie Farkas³ challenged the classical cannons by measuring the facial proportions of 200 women, including 50 models. His results concluded that some of the cannons are nothing more than artistic idealizations. Nevertheless, although social and cultural factors influence every generation's concept of beauty, the aesthetic cannons have withstood the test of time. Currently, the parameters established in the facial plastic surgery literature are based predominantly on the works of Powell and Humphreys, who in 1984 crystallized this topic into a single text *Proportions of the Aesthetic Face*.⁷

ANATOMIC LANDMARKS AND REFERENCE POINTS

Facial analysis is dependent on both soft-tissue and skeletal anatomic landmarks. Soft-tissue reference points are listed in Figure 21-3 and Box 21-1. Skeletal reference points are defined by cephalometric analysis and are listed in Figure 21-4 and Box 21-2.

The Frankfort horizontal plane (Figure 21-5) is the standard reference point for patient positioning in photographs and cephalometric radiographs. The Frankfort plane is defined as a line drawn from the superior aspect of the external auditory canal to the inferior border of the infraorbital rim while the patient's gaze is parallel to the floor. A soft-tissue definition for the inferior aspect of the infraorbital rim is the point of transition between lower eyelid and cheek skin.

FACIAL PROPORTIONS

The initial assessment of the face evaluates symmetry. Symmetry is rarely perfect when comparing halves through a midsagittal plane (Figure 21-6); nevertheless, midline points should lie on the axis line. Facial width is evaluated by dividing the face into equal fifths (Figure 21-7). The width of one eye should equal one

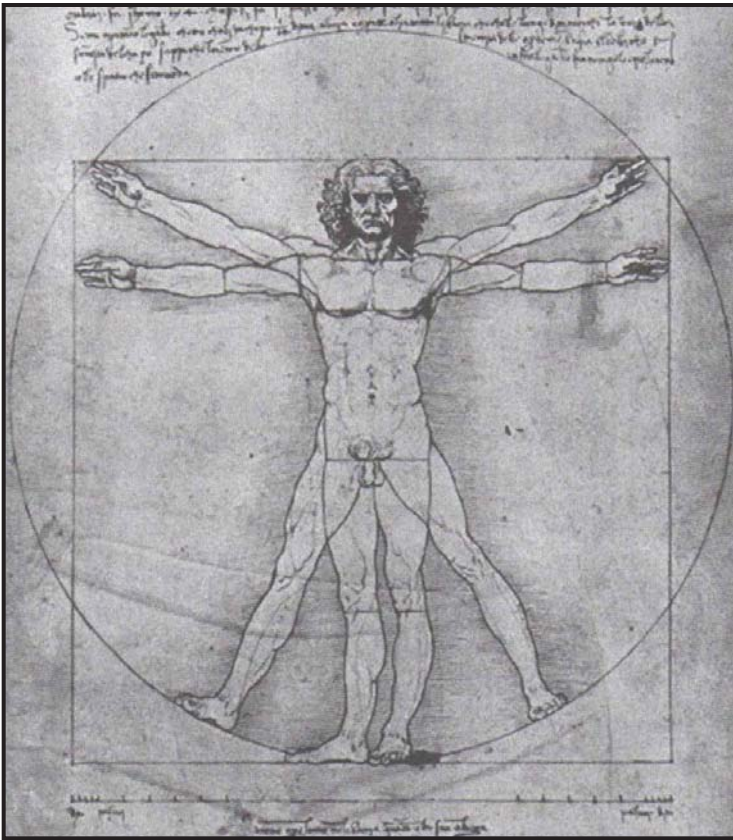


Figure 21-1. Leonardo da Vinci. The proportions of the body according to Vitruvius, ca. 1490. Pen and ink with touches of wash, over stylus 34.4 x 24.5 cm. (Courtesy of the Galleria dell' Accademia, inv.228, Venice.)

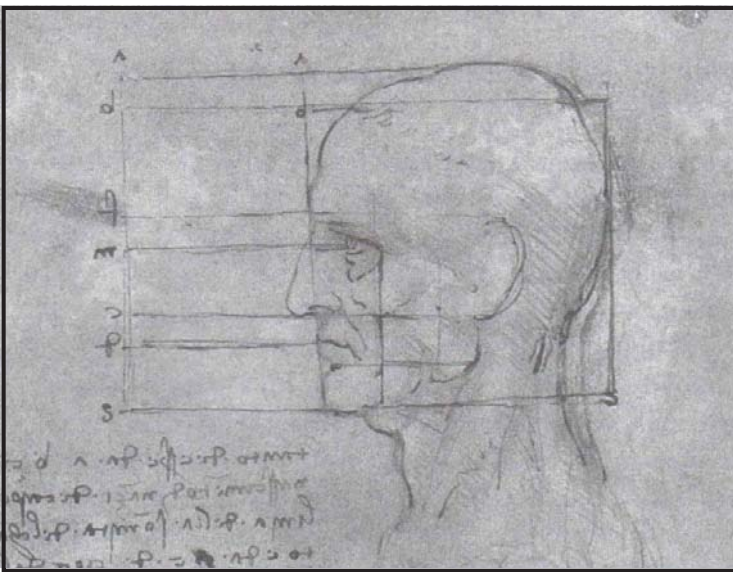


Figure 21-2. Leonardo da Vinci. The proportions of the head, ca. 1490. Pen and ink over black chalk, 28.0 x 22.2 cm. (Courtesy of the Galleria dell' Accademia, inv.236v, Venice.)

fifth of the total facial width, as well as the intercanthal distance or nasal base width.

Facial height is commonly assessed by one of two methods. The first method divides the face into equal thirds (Figure 21-8) as described by da Vinci. Measurements are made in the midline from the trichion to the glabella, from the glabella to the subnasale, and from the subnasale to the menton. The second method excludes the

upper third of the face because of common variability regarding hairline position. Measurements are made from the nasion (as opposed to the glabella) to the subnasale and from the subnasale to the menton (Figure 21-9). With this method the midface represents 43% of the height, with the lower face representing 57%.

SUBUNIT ANALYSIS

The face is divided into aesthetic units (Figure 21-10) that are further divided into subunits. The major units that are classically defined for facial analysis include the forehead, eyes, nose, lips, chin, ears, and neck. The units and subunits are based on skin thickness, color, texture, and underlying structural contour. Precise planning of surgical incisions and reconstructions require analysis of the entire unit or subunit. Incisions parallel to relaxed skin tension lines (Figure 21-11) and within unit or subunit borders result in the most favorable scars.

Forehead

The boundaries of the forehead are from the hairline to the glabella and make up the upper third of the face. The contour anatomy of the forehead is most aesthetically pleasing with a gentle convexity on profile. The nasofrontal angle (Figure 21-12) is created by a line tangent to the glabella through the nasion and intersecting with a line tangent to the nasal dorsum. The range of aesthetic measurements for this angle is from 115 to 135 degrees.

The ideal eyebrow shape follows a smooth and gently curving arc. The brow should begin medially with a slight clublike configuration and gradually taper toward its lateral end. Lateral position for a female is well above the supraorbital rim, whereas for a male it is at or close to the rim. The medial edge of the eyebrow lies on a perpendicular line that passes through the lateralmost portion of the nasal ala and approximately 10 mm above the medial canthus (Figure 21-13). In women, the highest point of the eyebrow arc is at a line drawn tangentially from the lateral limbus. However, this ideal eyebrow position can vary with fashion trends, and the highest point may actually lie anywhere from the lateral limbus to the lateral canthus. Sheens describes the eyebrow arc as most pleasing when it extends as an unbroken line from the brow down to the lateral nasal tip (Figure 21-14).

Eyes

The boundaries of the orbits are in the lower third of the upper face and the upper third of the midface. The width of one eye from medial to lateral canthus should equal one

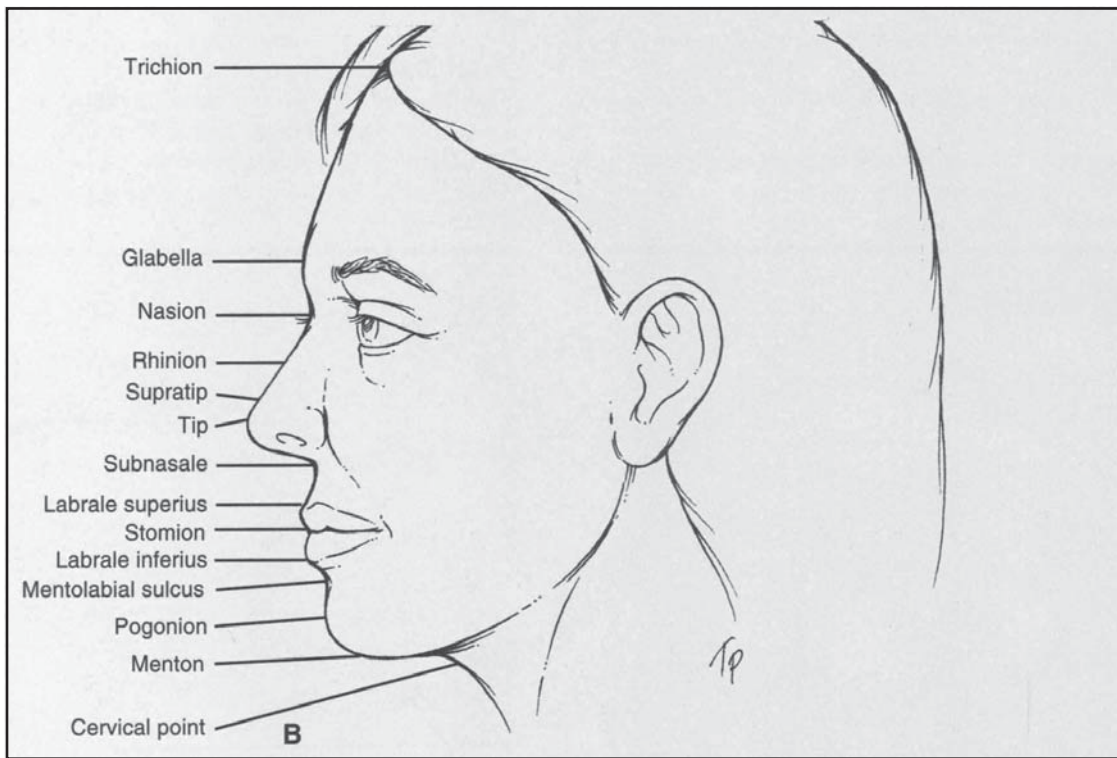
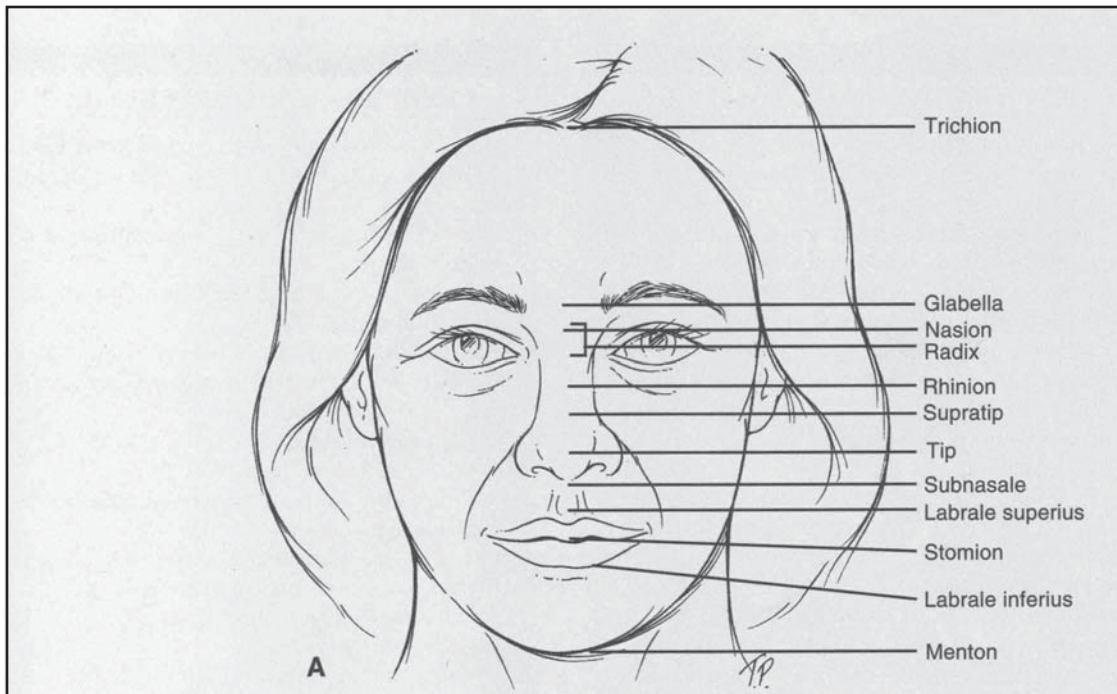


Figure 21-3. Soft Tissue reference Points.

fifth of the total facial width. The intercanthal distance should equal the width of one eye. Normal intercanthal distances for women and men are 25.5 to 37.5 mm and 26.5 to 38.7 mm, respectively. In general, the eye should be almond shaped with the lateral canthus slightly more superior than the medial canthus. The average palpebral opening is 10 to 12 mm in height and 28 to 30 mm in width. The upper lid crease is the line created by the inser-

tion of the levator aponeurosis and orbital septum into the orbicularis oculi and dermis. The location of the crease averages approximately 11 mm from the lash line but can vary between 7 and 15 mm. The upper eyelid normally covers a small portion of the iris but not the pupil. The lower eyelid is within 1 to 2 mm of the iris on neutral gaze, with the sclera not being visible below the iris margin.

SOFT TISSUE ANATOMIC LANDMARKS

Trichion (Tr): Anterior hairline in the midline
 Glabella (G): Most prominent point of the forehead on profile
 Nasion (N): The deepest depression at the root of the nose; typically corresponds to the nasofrontal suture
 Radix: Root of the nose, a region and not a point; part of an unbroken curve that begins at the superior orbital ridge and continues along the lateral nasal wall
 Rhinion (R): Soft-tissue correlate of the osseocartilaginous junction on the nasal dorsum
 Sellion: Osseocartilaginous junction on the nasal dorsum
 Supratip: Point cephalic to the tip
 Tip (T): Ideally, the most anterior projection of the nose on profile
 Subnasale (Sn): Junction of columella and upper lip
 Labrale superius (Ls): Vermilion border of upper lip
 Stomion (S): Central portion of interlabial gap
 Stomion superius: Lowest point of upper lip vermilion
 Stomion inferius: Highest point of lower lip vermilion
 Labrale inferius (Li): Vermilion border of lower lip
 Mentolabial sulcus (Si): Most posterior point between lower lip and chin
 Pogonion (Pg): Most anterior midline soft-tissue point of chin
 Menton (Me): Most inferior soft-tissue point on chin
 Cervical point (C): The innermost point between the submental area and the neck

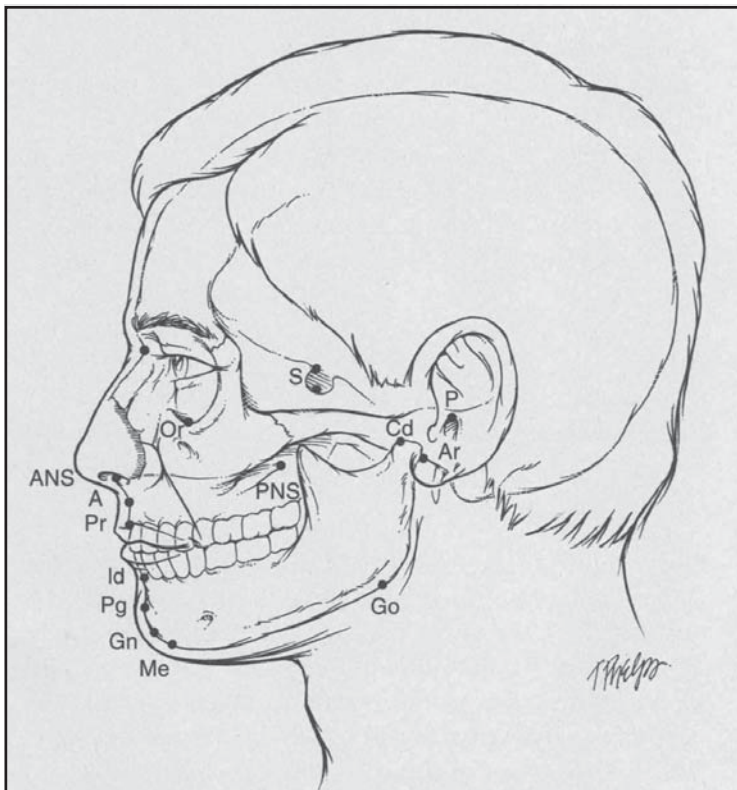


Figure 21-4. Cephalometric reference points.

CEPHALOMETRIC REFERENCE POINTS

(S) Sella: The midpoint of the hypophysial fossa
 (Or) Orbitale: The most inferior point on the infraorbital rim
 (P) Porion: The most superior point on the external auditory meatus
 (Cd) Condylion: The most superior point on the head of the mandibular condole
 (Ar) Articulate: The point of intersection of the posterior margin of the ascending mandibular ramus and the margin of the cranial base
 (ANS) Anterior nasal spine
 (PNS) Posterior nasal spine
 (A) Point A, subspinale: The deepest point in the concavity of the premaxilla
 (Pr) Prosthion: The lowest most anterior point on the alveolar portion of the premaxilla
 (Id) Infradentale: The highest most anterior point on the alveolar portion of the mandible
 (B) Point B, supramentale: The most posterior point in the outer contour of the mandibular alveolar process
 (Pg) Pogonion: Most anterior point on the bony chin in the midline
 (Gn) Gnathion: A point between the most anterior (Pg) and inferior (Me) point on the chin
 (Me) Menton: The lowest point on the mandible
 (Go) Gonion: The midpoint at the angle of the mandible

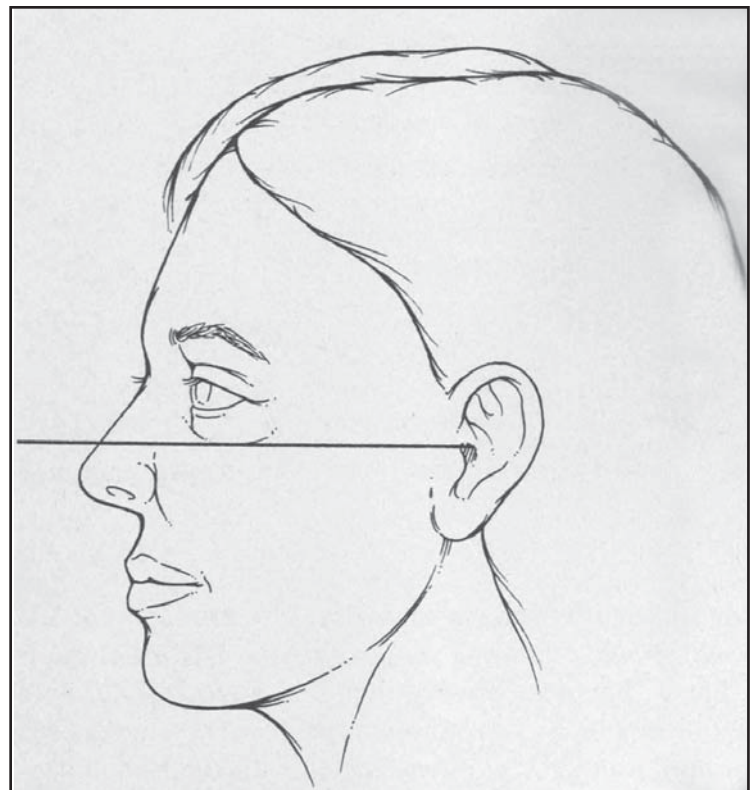


Figure 21-5. Frankfort horizontal plane. A line is drawn from the superior aspect of the external auditory canal to the most inferior aspect of the infraorbital rim.

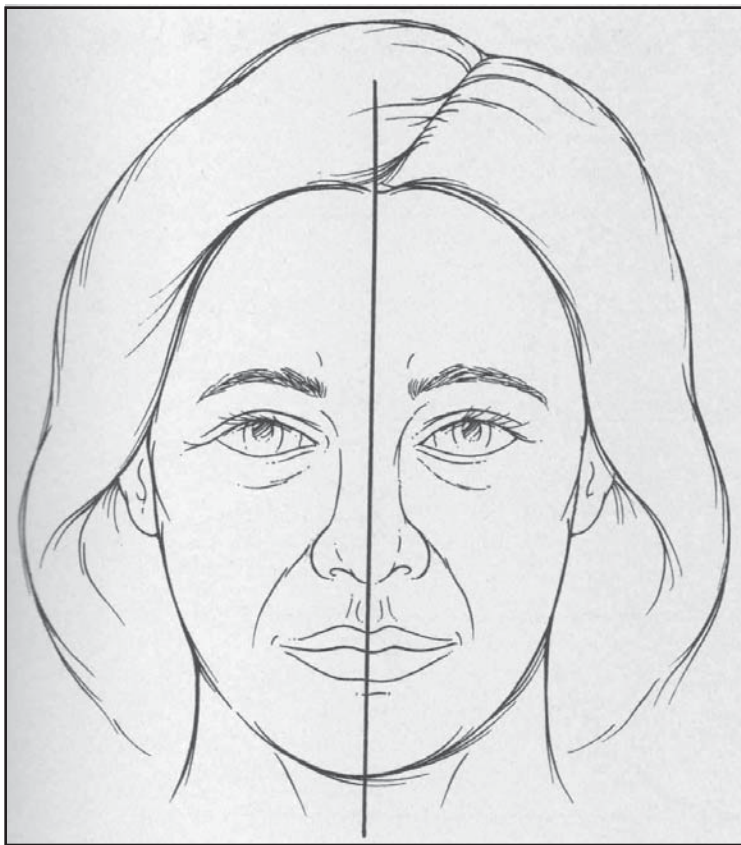


Figure 21-6. Facial symmetry through midsagittal plane.

Nose

The boundaries of the nose are within the middle third of the face. On the lateral view, the nasal starting point begins at the nasion, which ideally corresponds to the same level as the upper eyelid's superior palpebral fold (see Figure 21-3) and ends at the subnasale. Because the nose is the central and most prominent aesthetic unit of the face, it is always analyzed in relationship to other facial structures, most importantly the chin, lips, and eyebrows. The topographic subunits of the nose (see Figure 21-15) have been described by Burgett and are essential when planning reconstructive procedures. The borders of nasal subunits allow for scar camouflage when incisions lie along subunit margins.

Nasofacial Relationships

Powell and Humphreys' formulated relationships between the nose and face. They include the nasofrontal angle, nasolabial angle, nasofacial angle, and nasomental angle. The nasofrontal angle (see Figure 21-12) has been previously described in the forehead section of this chapter. The nasolabial angle defines the angular inclination of the columella as it meets the upper lip. The angle is formed between the intersection of a line tangent to the labrale superius and subnasale and a line tangent to the subnasale and the most anterior point of the columella (see Figure 21-16). This angle should measure 95 to 110 degrees in

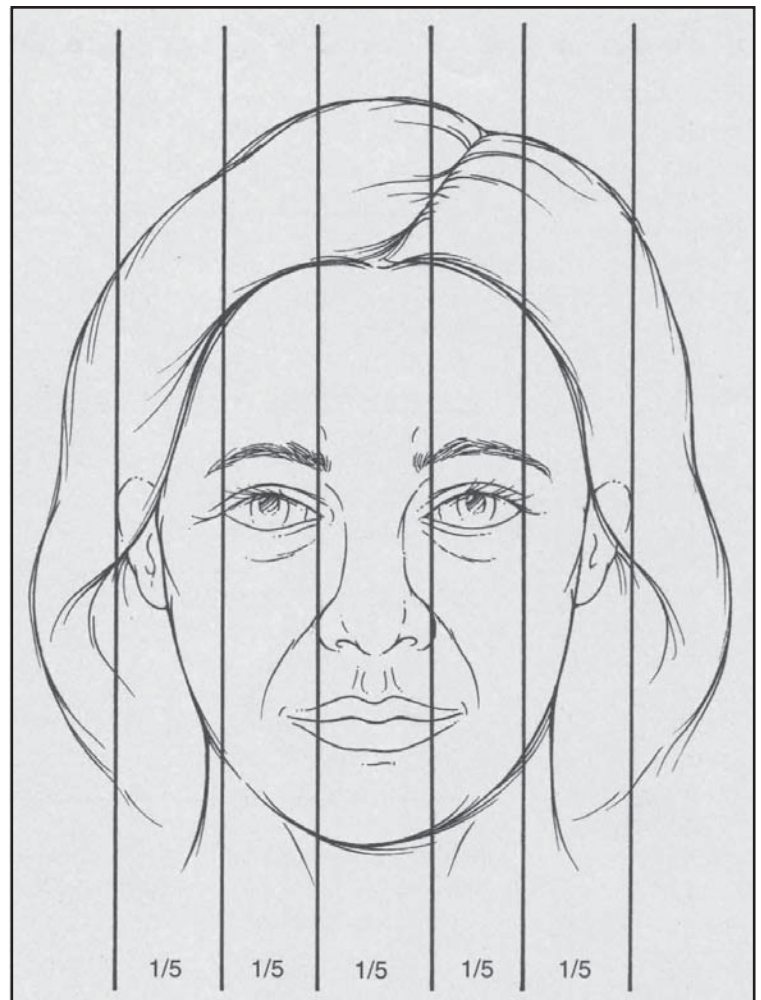


Figure 21-7. Facial Width. The facial width is divided into equal fifths.

women and 90 to 95 degrees in men. The nasofacial angle is the incline of the nasal dorsum in relation to the facial plane (see Figure 21-17). It represents the angle formed from a vertical line tangent from the glabella through the pogonion intersecting a line from the nasion through the nasal tip. This angle ideally measures 36 degrees but can vary from 30 to 40 degrees. The nasomental angle describes the angle between a tangent line from the nasion to the nasal tip intersecting with a line from the tip to the pogonion (see Figure 21-18). The range of this angle is from 120 to 132 degrees, and it can clearly be obscured if the chin or lip position is in facial disharmony.

Nasal Rotation and Projection

Nasal rotation and projection are essential measurements in determining nasal aesthetics. Tip rotation generally occurs along an arc produced by a radius based at the external auditory canal (Figure 21-19). Rotation increases along the upper portion of the arc and decreases along the lower portion. Several methods have been used to analyze tip projection and, in turn, have defined nasal length. Simons⁹ measures tip projection in relation to the length

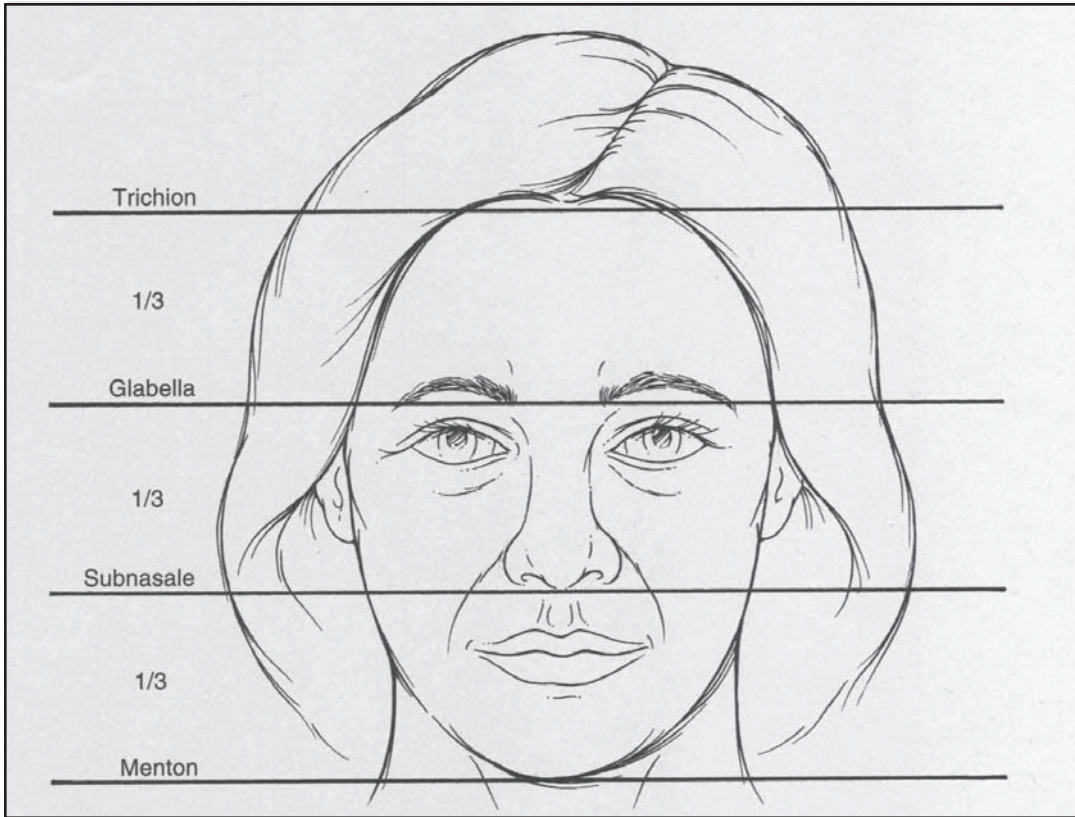


Figure 21-8. Facial height. The facial height is divided into equal thirds. From trichion to glabella, from glabella to subnasale, and from subnasale to menton.

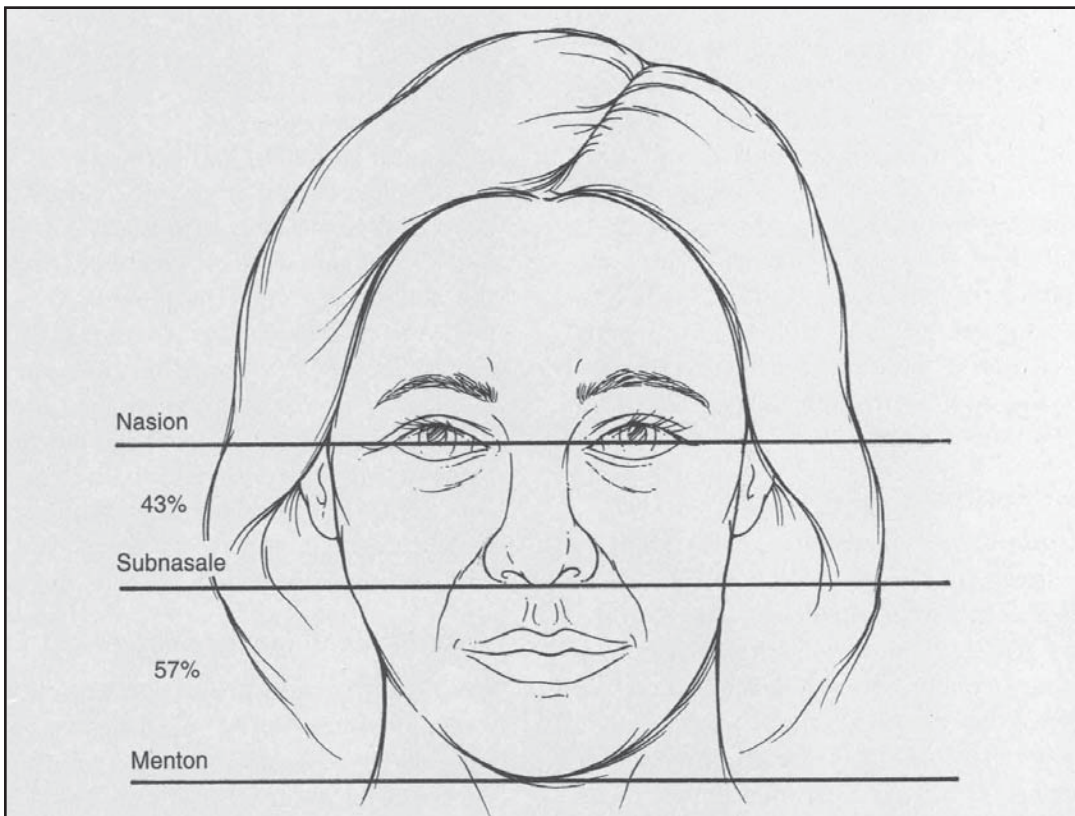


Figure 21-9. Middle and lower facial height. Division of height is unequal and measured from the nasion to subnasale and from the subnasale to the menton.

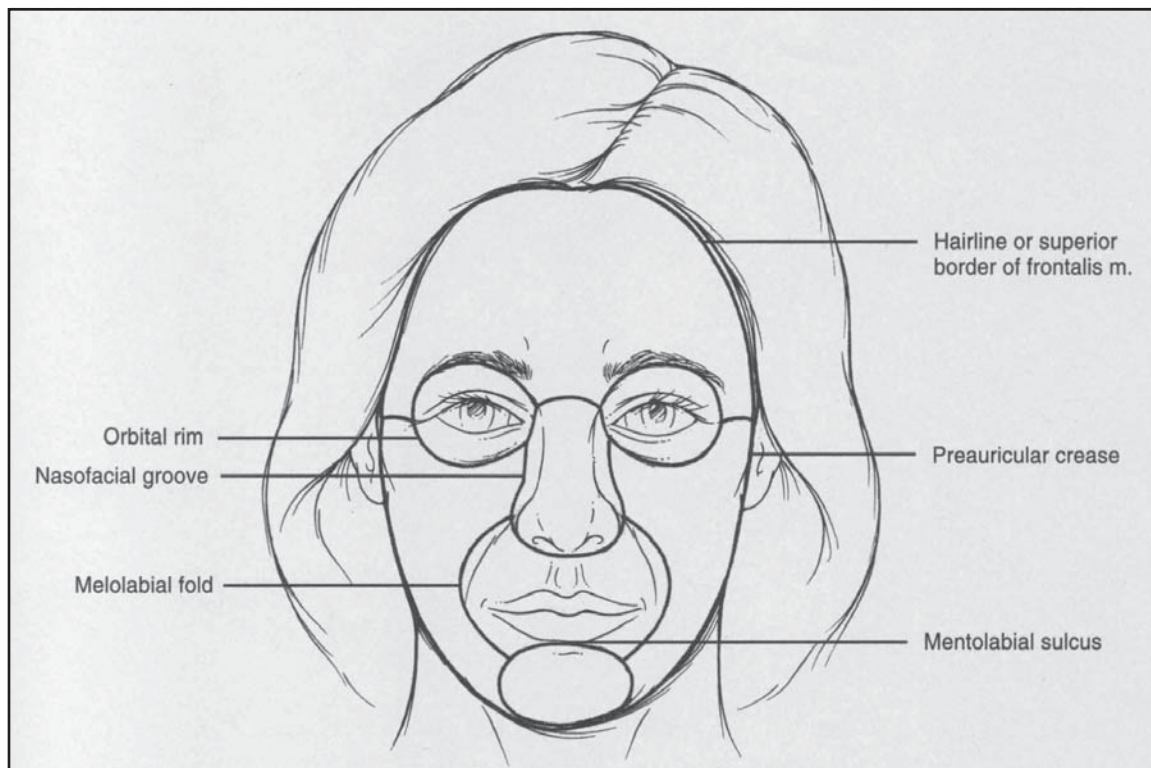


Figure 21-10. Aesthetic units of the face

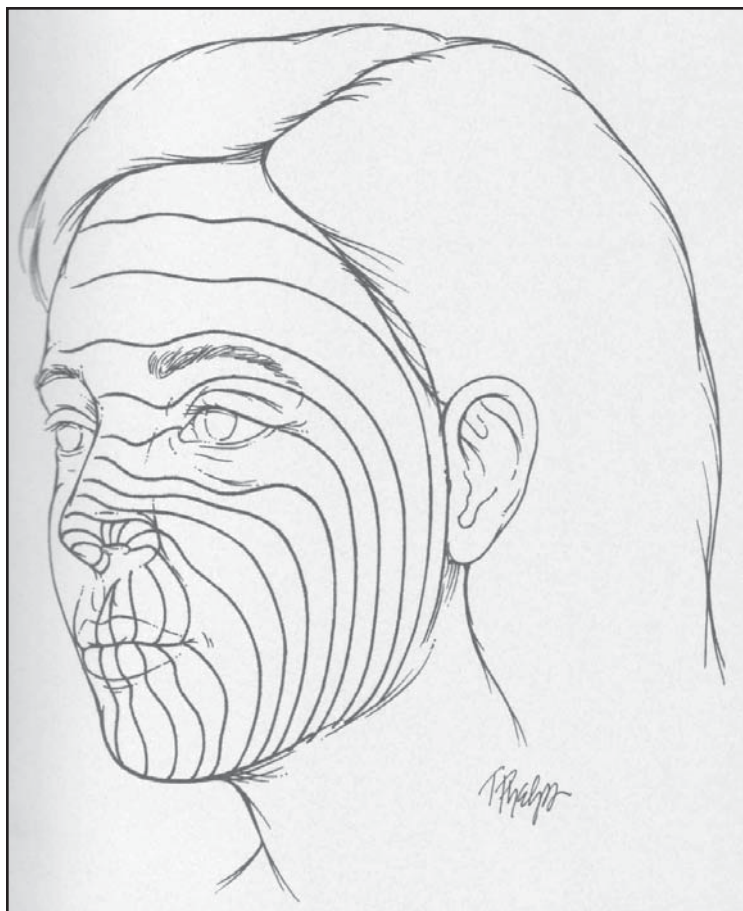


Figure 21-11. Relaxed skin tension lines (RSTL) of the face.

projection in relation to the length of the upper lip (see Figure 21-20). Nasal projection is approximately equal to the length of the upper lip, giving a ratio of 1:1. Goode's⁷ method uses a vertical line drawn from the nasion to the alar groove, a perpendicular line from the alar groove to

the nasal tip, and a line from the tip back to the nasion (see Figure 21-21). The ratio comparing the length of the perpendicular line (alar groove to tip) with that of the nasal length (nasion to tip) should be 0.55 to 0.60. When these ratios are observed, the nasofacial angle is approximately 36 degrees. Crumley² uses a similar method and uses a 3-4-5 triangle, where the hypotenuse is the nasal length and the projection is the smallest arm of the triangle.

Alar-Columellar Complex

On lateral view, the ala-to-tip lobular complex ratio is considered optimal at 1:1 (see Figure 21-22, A). Columella show of 3 to 5 mm is considered acceptable (see Figure 21-22, B). From the basal view, the nose should be triangular in shape and divided into three equivalent units (see Figure 21-23).

Lips

The boundaries of the lips are contained within the lower one third of the face. The upper lip is measured from the subnasale to the stomion superius, whereas the lower lip and chin are measured from the stomion inferius to the menton (see Figure 21-24). The subunits of the lip are well defined (see Figure 21-25), whereas the height of the upper lip to the lower lip should have a ratio of approximately 1:2. Horizontal lip position can be determined by two separate methods. The first constructs a line from the

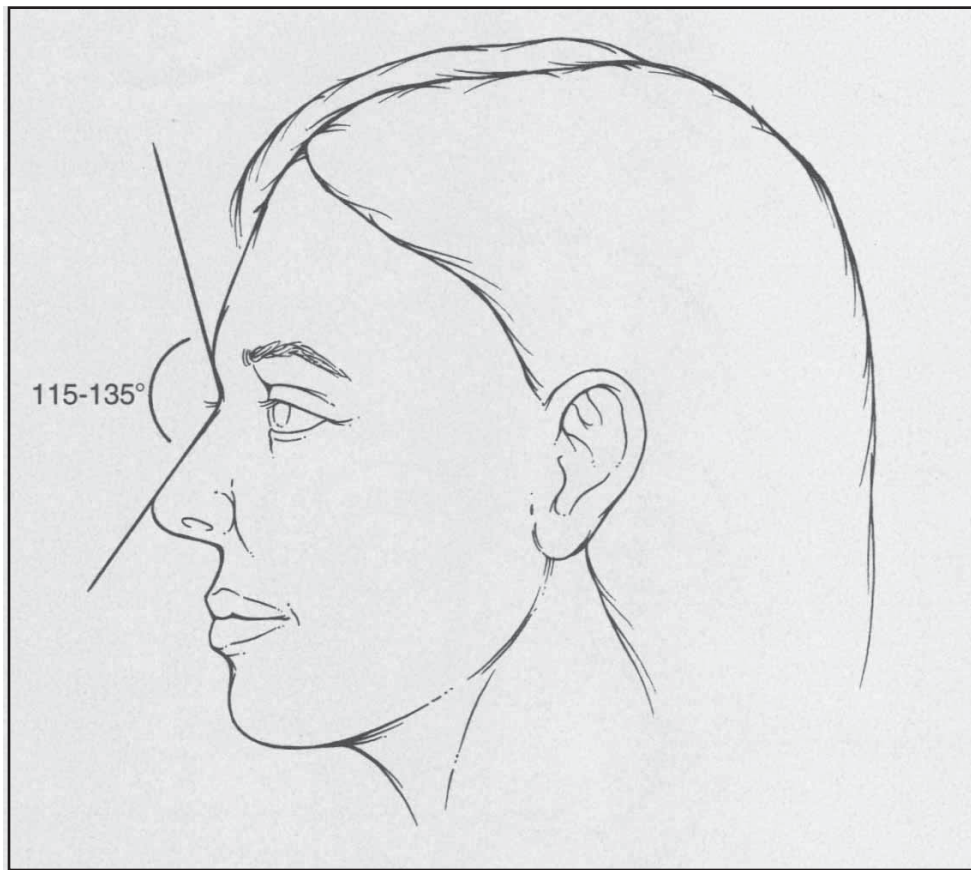


Figure 21-12. Nasofrontal angle (115-135 degrees)

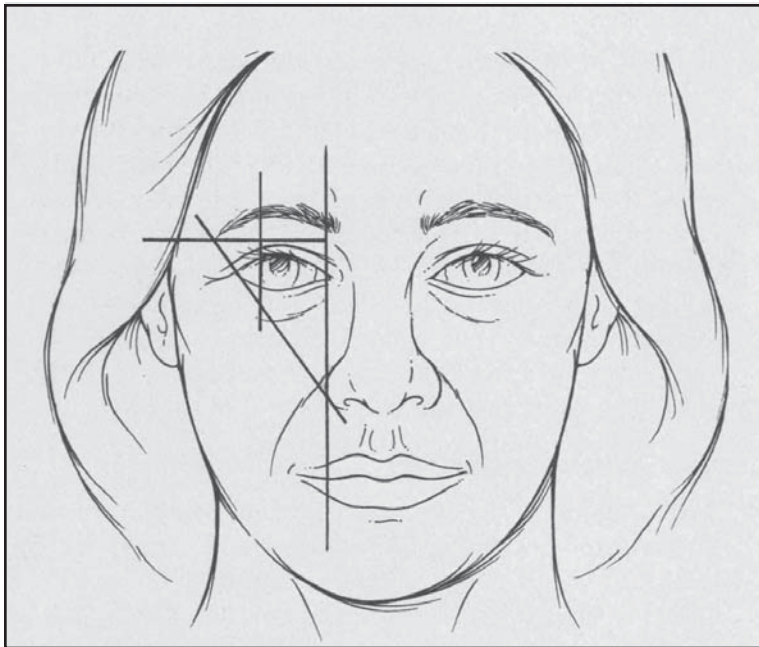


Figure 21-13. Ideal eyebrow position. Medial brow head lies along horizontal tangent with medial canthus and nasal ala. Highest point of brow arch is located above lateral limbus.

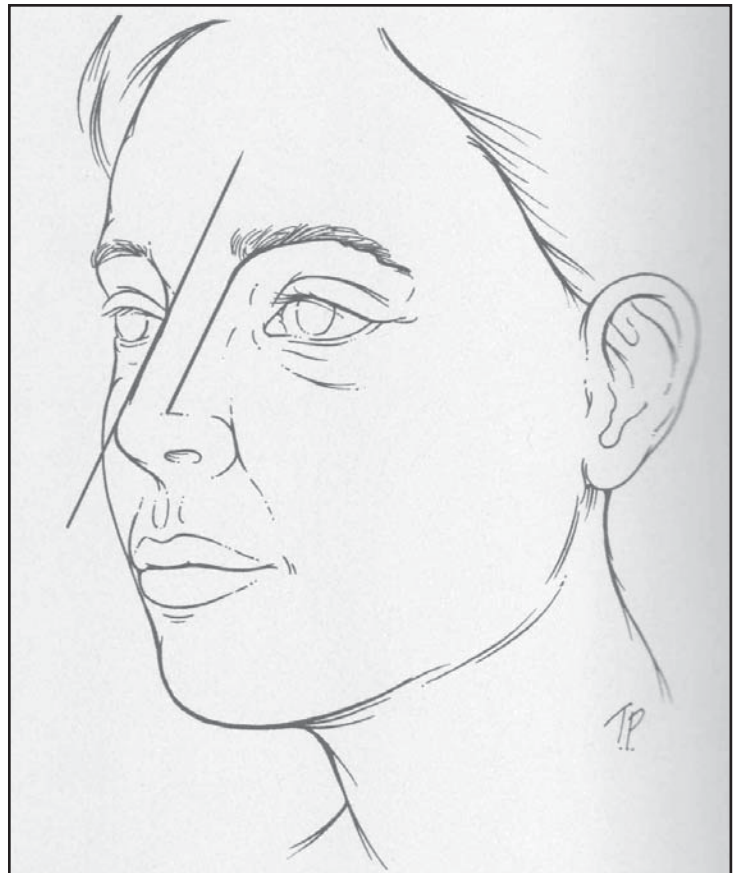


Figure 21-14. Unbroken aesthetic line form eyebrow to nasal tip.

subnasale through the labrale inferius to the pogonion (see Figure 21-26). A perpendicular line through the anterior-most point of each lip defines its horizontal position. The upper and lower lip should lie 3.5 and 2.2 mm anterior to this line, respectively. The second method uses the nasomental angle to determine horizontal lip position.

The lips should fall just behind this line at a distance of 4 mm for the upper lip and 2 mm for the lower lip (see Figure 21-18).

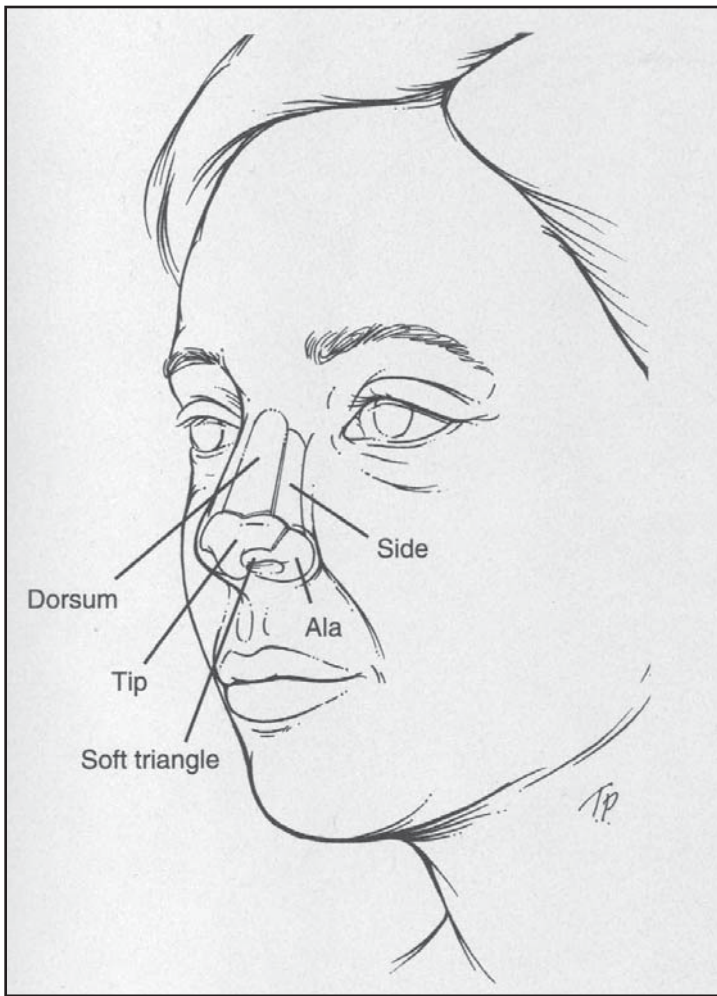


Figure 21-15. Nasal aesthetic subunits adapted from Burget.

Chin

The boundaries of the chin lie in the lower one third of the face and can be measured from the mentolabial crease to the menton. The chin is a pivotal facial unit when analyzing the nose or neck. Most rhinoplasty analysis begins

with proper chin position in relation to nasal projection and facial harmony. Gonzales Ulloa⁶ described the ideal chin position by a tangential line through the nasion to pogonion, which is almost perpendicular to the Frankfort horizontal plane (see Figure 21-27). An alternative method for analyzing chin position has already been described in the lip section (see Figure 21-26), where the mentolabial sulcus lies approximately 4 mm behind this line.

Neck

The ideal neck has a well-defined mandible from the pogonion to the angle with an acute mentocervical angle. This angle is produced by drawing a line from the glabella to the pogonion and intersecting with a line tangent from the menton to the cervical point (see Figure 21-28). The cervical point is defined as the innermost point between the submentum and neck. It is also important to evaluate chin position when analyzing the neck, because an obtuse mentocervical angle may cause the perception of poor chin projection.

Ears

The width of the ear is approximately one half its length. The ear length should approximate the length of the nose measured from the nasion to the subnasale. The superior aspect of the ear lies at the level of the eyebrow, whereas its inferior aspect is at the level of the nasal ala. The long axis of the ear is parallel to the long axis of the nasal dorsum (see Figure 21-29) and is noted to have a posterior rotation of approximately 15 degrees from the vertical

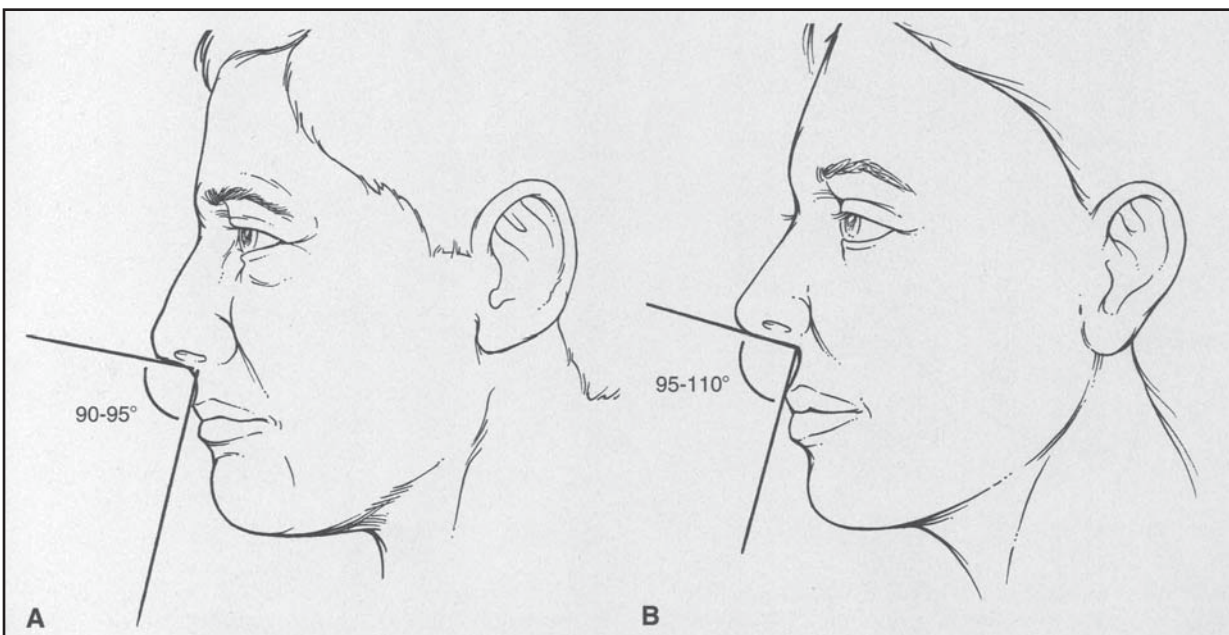


Figure 21-16. Nasolabial angle. Male, 90 to 95 degrees; female, 95 to 110 degrees.

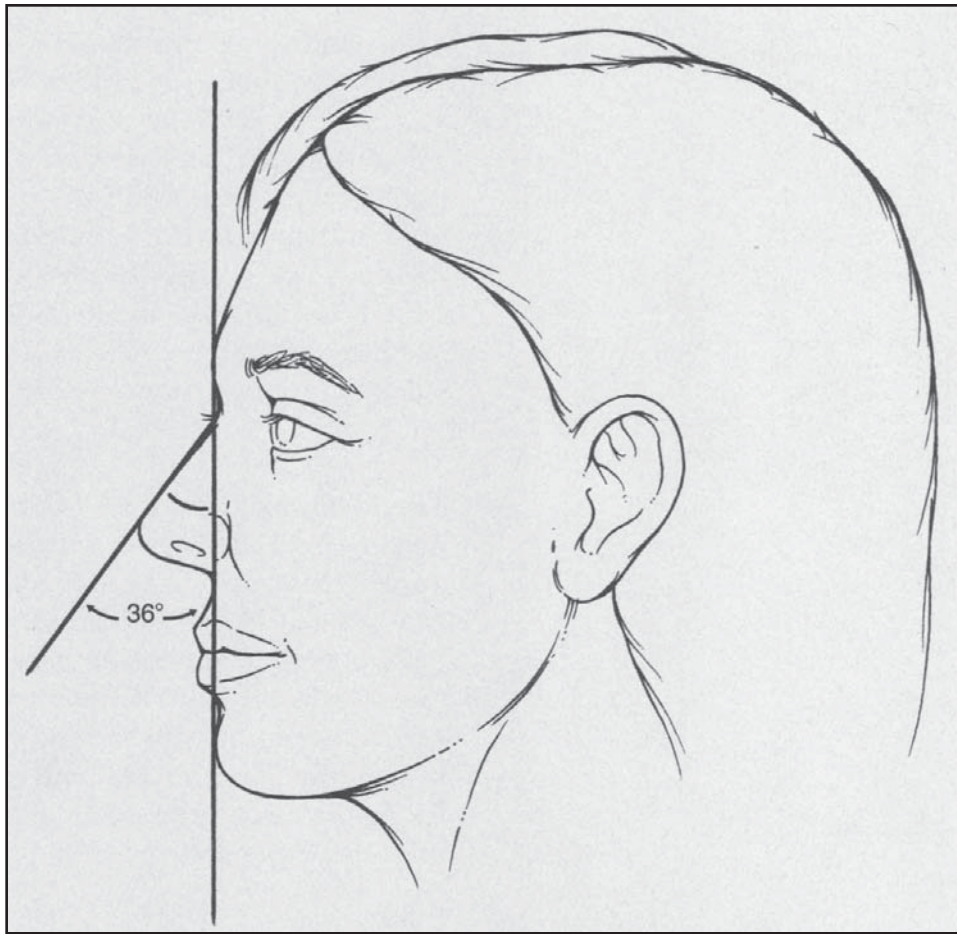


Figure 21-17. Nasofacial angle (30 to 40 degrees).

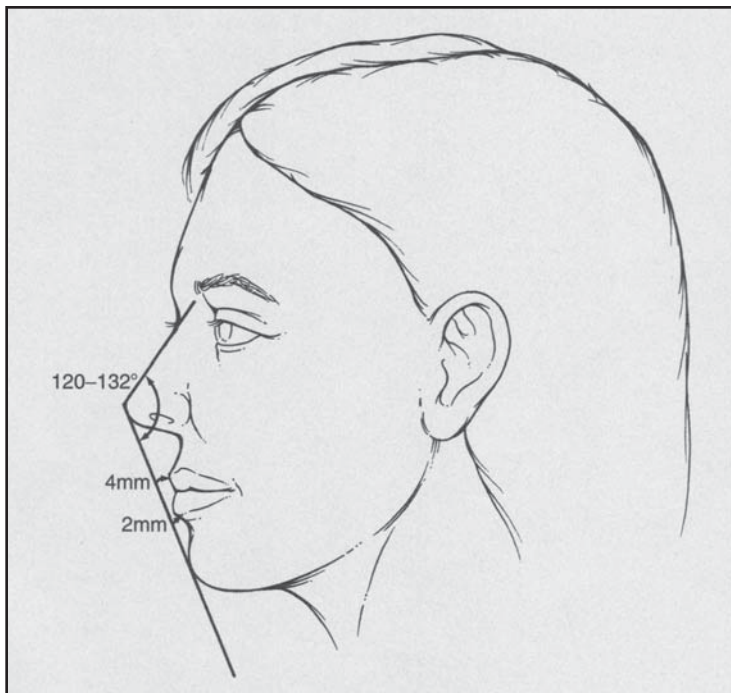


Figure 21-18. Nasomental angle (120-132 degrees). The lips should fall just behind this line at a distance of 4 mm for the upper lip and 2 mm for the lower lip.

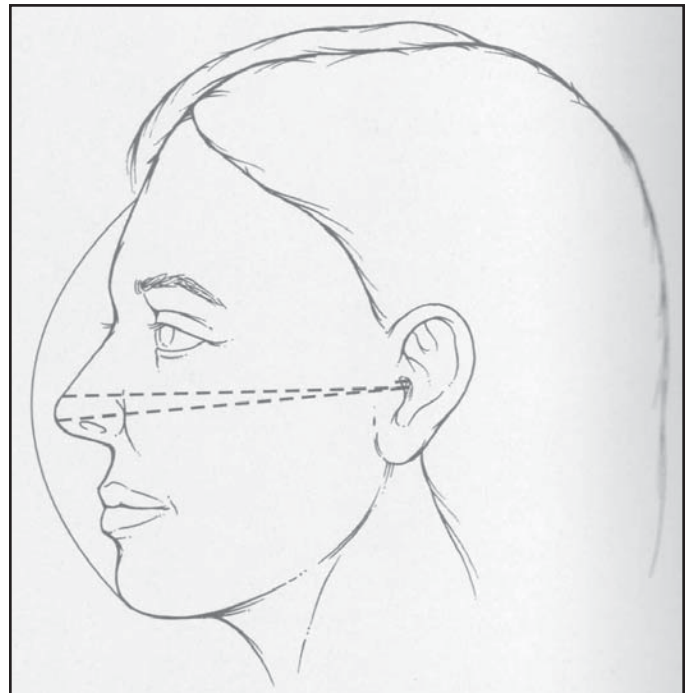


Figure 21-19. Tip rotation generally occurs along an arc produced by a radius based at the external auditory canal.

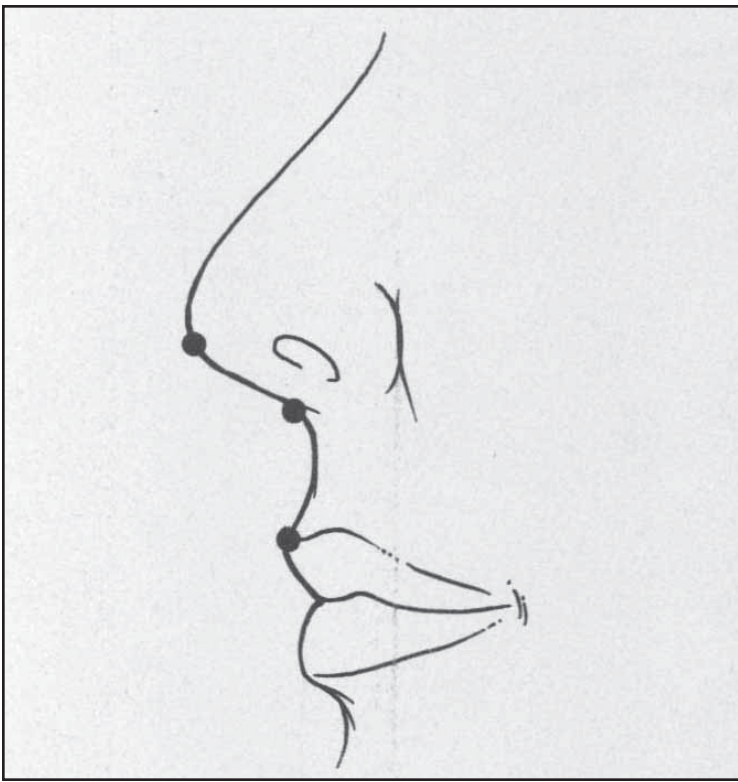


Figure 21-20. Simon's nasal projection is approximately equal to the length of the upper lip with a ratio of 1:1.

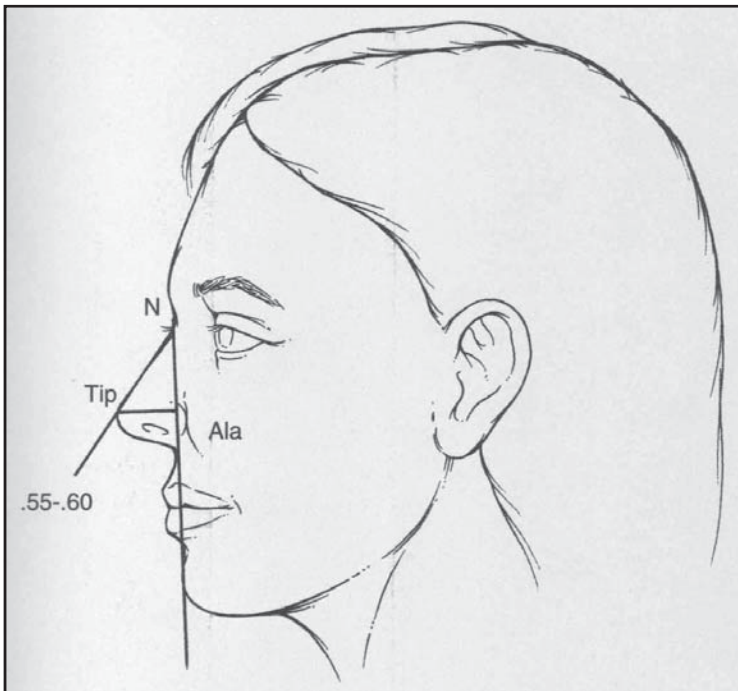


Figure 21-21. Goode's method of tip projection.

plane. The ear protrudes from the skull at an angle of approximately 20 to 30 degrees, which usually translates into a measurement of 15 to 25 mm from the helix to the mastoid skin.

Skin and Rhytids

When analyzing the face, evaluation of the skin deserves special attention. Skin texture, thickness, elasticity, and solar damage are all critical factors contributing to one's overall facial appearance. In 1988, Fitzpatrick⁴

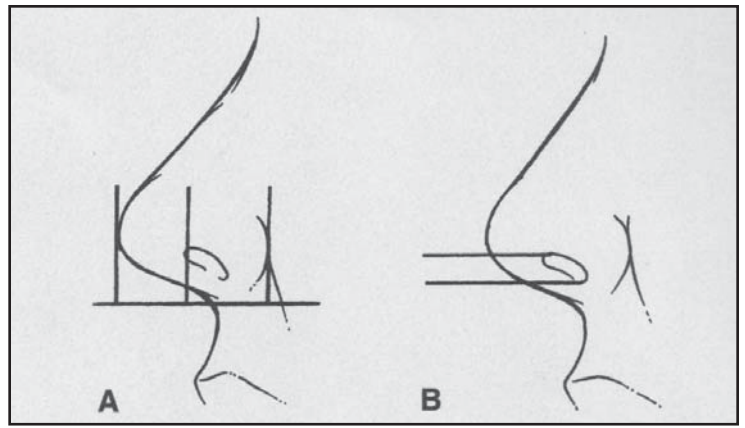


Figure 21-22. Nasal ala. Ala-to-tip lobular ratio should be 1:1. Columella shown between 3 and 5 mm.

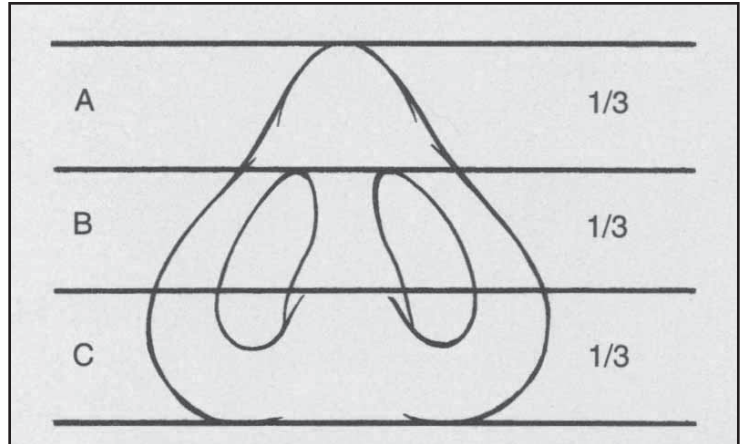


Figure 21-23. Nasal base divided into equal thirds.

established skin type classification (Box 21-3), and in 1994, Glogau⁵ categorized photoaged skin (see Box 21-4). Most importantly, however, in the examination of the skin is the analysis of facial rhytids. Wrinkles or rhytids originate from a wide variety of sources that can include chronologic aging, photoaging or solar damage, and skin folding secondary to loss of underlying skeletal or soft tissue support. Hyperdynamic facial lines (see Figure 21-30) are specific wrinkles that are caused by long-term facial muscle animation. Examples of these include horizontal forehead creases, crow's feet, and glabellar lines. Each line is caused by repeated underlying muscle contraction. Hyperdynamic lines should be distinguished from other facial lines such as the melolabial fold, mentolabial sulcus, and the fine crisscross wrinkling found on the cheek and under the eyelids.

COMPUTER IMAGING AND DIGITAL PHOTOGRAPHY

Technologic advances in digital photography and computer graphics have revolutionized the way many surgeons obtain and process patient photographs. The immediate availability of photographs for review and the ability to generate computer-modified images provide an easy and effective means of preoperative analysis. Routine office consultations typically include

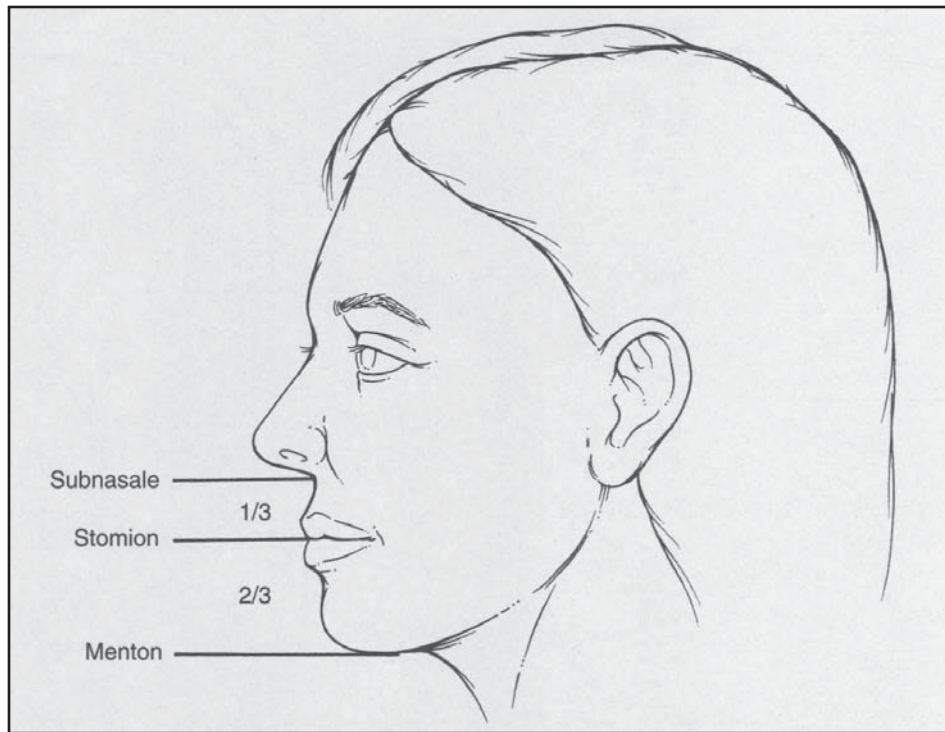


Figure 21-24. Lip ratio and lower facial third.

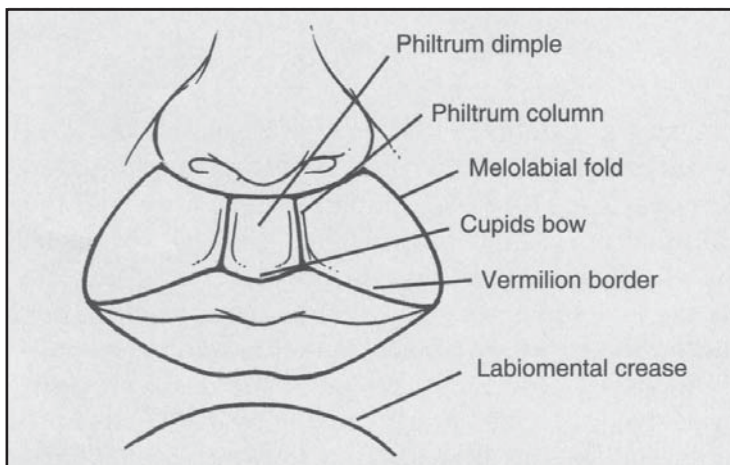


Figure 21-25. Lip aesthetic subunits.

"patient imaging," which has become a vital tool toward preoperative education. It provides the surgeon an opportunity to strengthen communication with the patient regarding realistic expectations of surgical outcome. Added benefits of computer imaging also include photo-archiving and its use as an instructional tool for residents and fellows. Over the past few years, this technology has evolved from being costly, cumbersome, and slow to one that is highly efficient, user-friendly, and reasonably priced.

The essential components for a computer imaging system include a computer, an image capture device or camera, and imaging software. Computer specifications

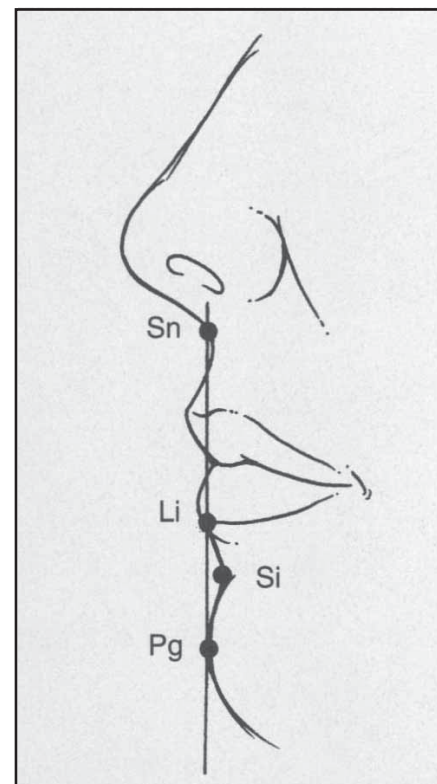


Figure 21-26. Horizontal lip position. Mentolabial sulcus (Si) should lie 4 mm posterior to a vertical line dropped from the subnasale through the labrale inferius (Li) and extending to the pogonion (Pg).

are dependent on the demands and expectations of the surgeon; however, current system requirements needed to operate high-end digital imaging software include a Pentium III processor, 256-MB RAM, a 32-bit graphics card, and a minimum of a 40-MB hard drive. Additional components that are highly recommended

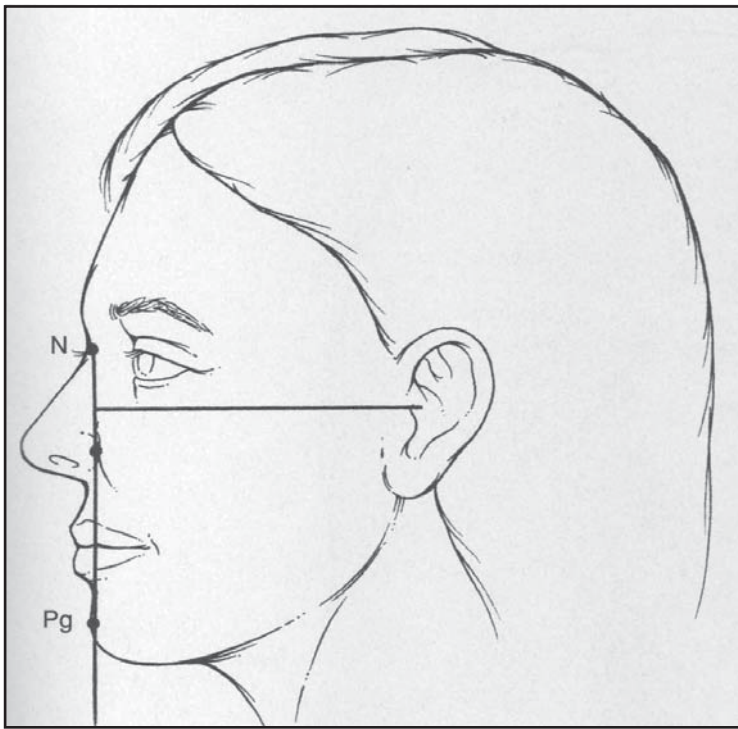


Figure 21-27. The zero meridian of Gonzalez-Ulloa. Ideal chin position is on a vertical line from the nasion (N) to the pogonion (Pg), which is perpendicular to the Frankfort horizontal.

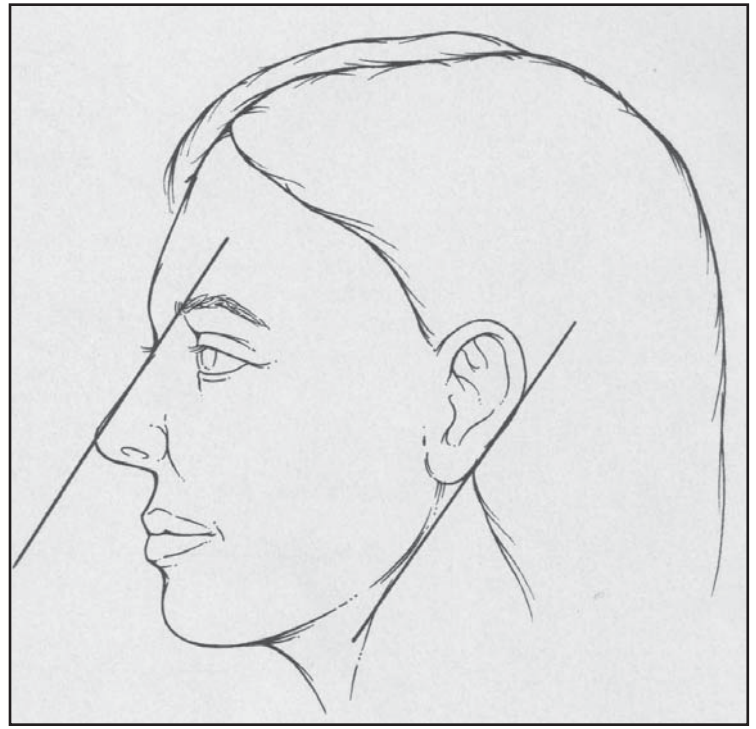


Figure 21-29. Long axis of the ear parallels the long axis of the nasal dorsum.

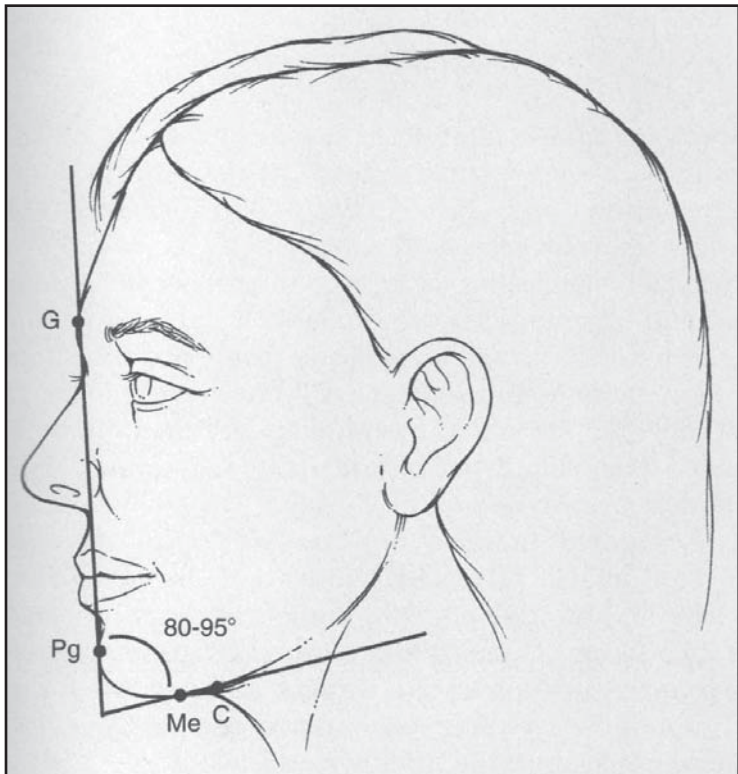


Figure 21-28. Mentocervical angle (80-95 degrees).

include a CD burner for archiving and storage, a graphics board, digital drawing tablet, and a high-resolution color printer.

As with 35-mm photography, the clarity of digital photography is dependent on the sophistication of

BOX 21-3		
FITZPATRICK CLASSIFICATION OF SUN-REACTIVE SKIN TYPE		
Skin type	Skin color	Characteristics
I	White	Always burns, never tans
II	White	Usually burns, tans with difficulty
III	White	Sometimes burns, sometimes tans
IV	White	Rarely burns, tans with ease
V	Brown	Very rarely burns, tans very easily
VI	Black	Never burns, always tans

BOX 21-4
GLOGAU PHOTOAGING CLASSIFICATION
Type I: No keratoses, few wrinkles, age 20 to 30, rarely wears makeup
Type II: Early lentigenes, wrinkles on animation, age 30 to 40, sometimes wears makeup
Type III: Advanced photoaging, wrinkles present at rest, age 50 to 60, always wears makeup
Type IV: Severe photoaging, severe wrinkling, age 60 to 70, makeup has minimal benefit

the camera and its lens. The resolution of digital cameras is described in pixels, and it currently ranges up to 6.0 mega pixels. However, a camera containing 3.0 mega pixels is sufficiently suited for the demands

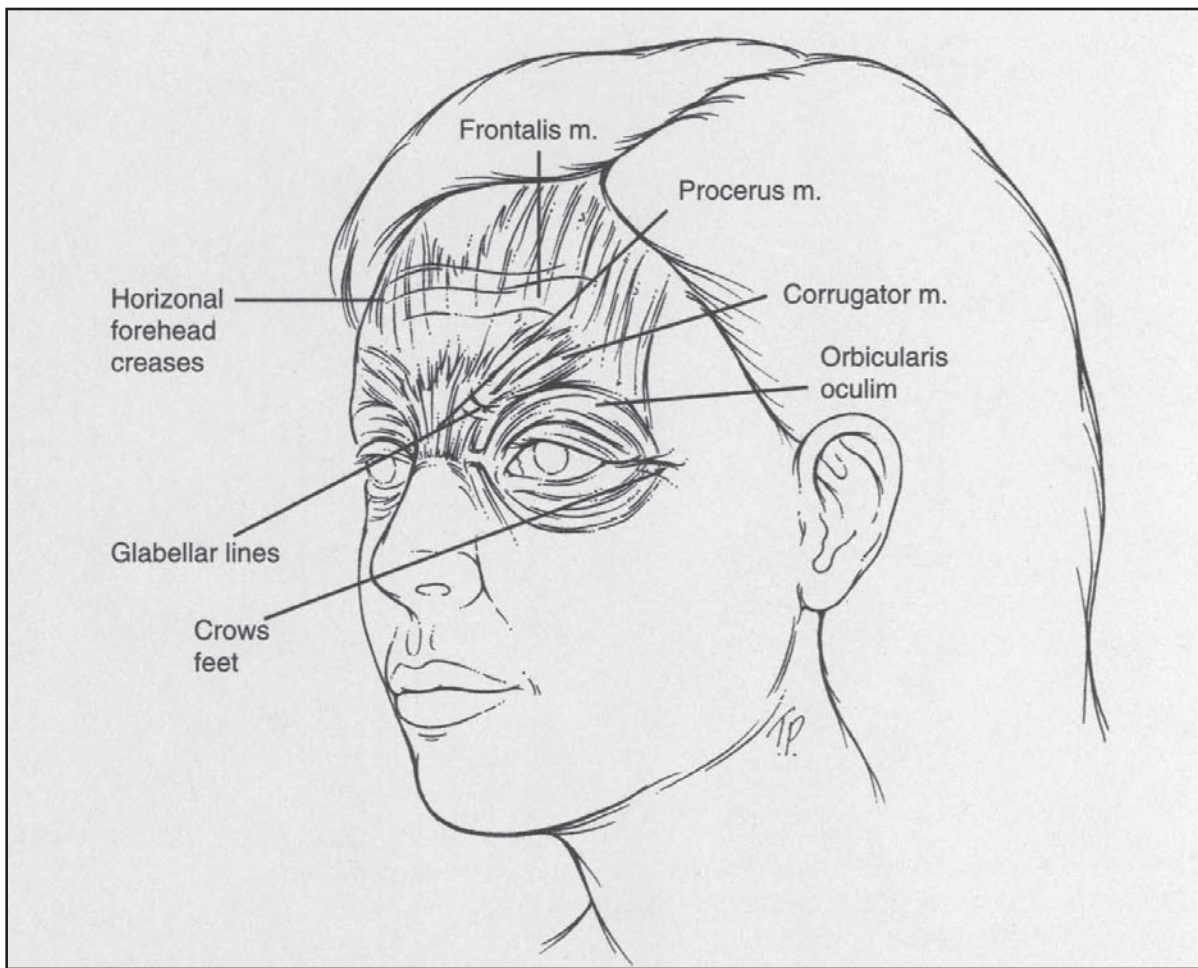


Figure 21-30. Hyperdynamic facial lines caused by repeated underlying muscle contraction.

of most medical photography. A 3.0-mega pixel image printed on 4 x 6-inch glossy photo paper is nearly indistinguishable from a conventional photograph. The Nikon Coolpix 4500 and the Canon G3 Powershot are examples of high-end consumer "point-and-shoot" cameras. These 4.0-mega pixel digital cameras cost less than \$1000 and would satisfy most surgeon's needs. For a more professional look with 35-mm like quality and control, the Fuji FinePix S2 Digital Camera is a true single lens reflex (SLR) with 6.0 mega pixels (see Figure 21-31). The additional capabilities include interchangeable lenses and through-the-lens (TTL) metering. The price for advanced digital cameras has dropped dramatically over the past several years, and they can now be purchased for as little as \$2000 to \$3000. Lighting, background, and patient positioning are similar to conventional photography with 35-mm cameras.

Once the photograph images are downloaded onto the computer, a variety of image or graphics software may be used to open and alter images. The Mirror Suite (Image Management plus Simulation) (Canfield Scientific, Inc., Fairfield, NJ) is sophisticated but user-friendly high-end software designed for medical professionals. Image files from the camera once downloaded are automatically tethered into the Mirror Software and saved into patients'

charts. The ease and speed of image alteration lies at the heart of this sophisticated software, making patient consultations streamline and informative. Furthermore, this advanced software has the ability to measure and analyze facial angles for assistance in preoperative analysis and planning (see Figure 21-32). The cost of such commercially available systems, complete with computer, camera, and software will be several thousands of dollars. More basic systems, however, may be pieced together by a physician to maintain a more modest price point.

Computer imaging and its ability to generate altered images for patient education can be particularly helpful during the preoperative rhinoplasty consultation. Computer-generated changes are compared with preoperative images and reviewed with the patient. The surgeon must be conservative with computer-generated changes and avoid overzealous alterations. In this manner, realistic expectations are nurtured, and a common outcome concept can be reached between surgeon and patient. Computer imaging can be particularly helpful to demonstrate to the rhinoplasty patient with microgenia the added benefit of chin augmentation (see Figure 21-33). The computer-generated images assist patients in visualizing the overall improvement in facial harmony.

FUJI S2 PRO

Professional Digital SLR camera

- 6.1MP Fujifilm SuperCCD
- TTL metering
- 1.8" LCD display
- Compatible with most F-mount Nikkor lenses
- Accepts CompactFlash, SmartMedia or IBM MicroDrive
- FireWire and USB interface



Paired with the Canfield TwinFlash, the Fuji S2 is ideal for everything from close-ups to body photos

Figure 21-31. Fuji S2 pro digital SLR camera with Canfield twin flash.

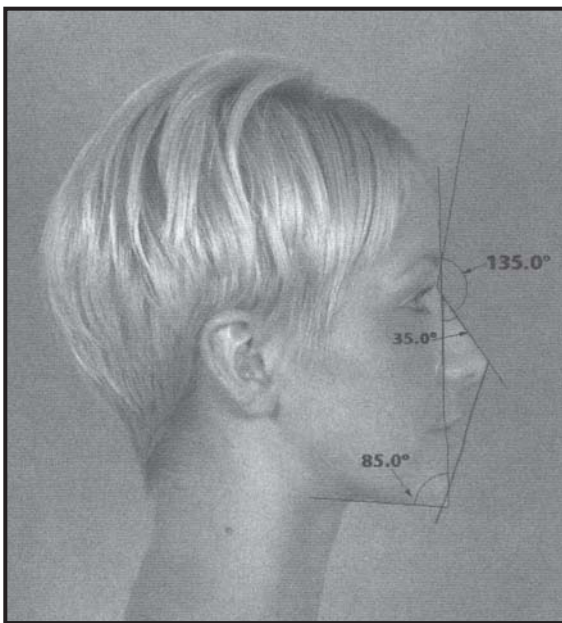


Figure 21-32. Facial angle analysis, including nasofrontal angle, nasofacial angle, and mentocervical angle. (Courtesy of Canfield Clinical Systems.)



Figure 21-33. Preoperative (left) and postcomputer imaging (right) of combined Rhinoplasty and chin augmentation. (Courtesy of Canfield Clinical Systems.)

REFERENCES

1. Burget GC: Aesthetic restoration of the nose, *Clin Plast Surg* 12:463, 1985.
2. Crumley RL, Lanser M: Quantitative analysis of nasal tip projection, *Laryngoscope* 98:202, 1988.
3. Farkas LG and others: Vertical and horizontal proportions of the face in young adult North American Caucasians: revision of neoclassical canons, *Plast Reconstr Surg* 75:328, 1985.
4. Fitzpatrick TB: The validity and practicality of sun reactive skin types I through VI, *Arch Dermatol* 124:869, 1988.
5. Glogau RG: Chemical peeling and aging skin, *J Geriatr Dermatol* 2:30, 1994.
6. Gonzalez-Ulloa M: Quantitative principles in cosmetic surgery of the face (profileplasty), *Plast Reconstr Surg* 29:186, 1962.
7. Powell N, Humphreys B: Proportions of the aesthetic face, New York, Thieme-Stratton, 1984.
8. Sheen JH: Aesthetic rhinoplasty, St. Louis, Mosby, 1978.
9. Simons RL: Nasal tip projection, ptosis and supratip thickening. *Ear Nose Throat J* 61:452, 1982.

For More Information visit www.marczimplermd.com